Giardia muris Infection in Mice Is Associated with a Protective Interleukin 17A Response and Induction of Peroxisome Proliferator-Activated Receptor Alpha

Leentje Dreesen,[a] Karolien De Bosscher,[b] Grietje Grit,[a] Bart Staels,[c] Erik Lubberts,[d] Eric Bauge,[c] Peter Geldhof[a]

Department of Virology, Parasitology and Immunology, Faculty of Veterinary Medicine, Ghent University, Merelbeke, Belgium[a]; Laboratory of Eukaryotic Gene Expression & Signal Transduction, Department of Biochemistry, Ghent University, Ghent, Belgium[b]; Université Lille 2, INSERM U1011, European Genomic Institute for Diabetes (EGID), and Institut Pasteur de Lille, Lille, France[c]; Department of Rheumatology, Erasmus University Medical Center, Erasmus University, Rotterdam, The Netherlands[d]

The protozoan parasite *Giardia duodenalis* (*Giardia lamblia*) is one of the most commonly found intestinal pathogens in mammals, including humans. In the current study, a *Giardia muris*-mouse model was used to analyze cytokine transcription patterns and histological changes in intestinal tissue at different time points during infection in C57BL/6 mice. Since earlier work revealed the upregulation of peroxisome proliferator-activated receptors (PPARs) in *Giardia*-infected calves, a second aim was to investigate the potential activation of PPARs in the intestines of infected mice. The most important observation in all mice was a strong upregulation of *il17a* starting around 1 week postinfection. The significance of interleukin 17A (IL-17A) in orchestrating a protective immune response was further demonstrated in an infection trial or experiment using IL-17 receptor A (IL-17RA) knockout (KO) mice: whereas in wild-type (WT) mice, cyst secretion dropped significantly after 3 weeks of infection, the IL-17RA KO mice were unable to clear the infection. Analysis of the intestinal response further indicated peroxisome proliferator-activated receptor alpha (PPARα) induction soon after the initial contact with the parasite, as characterized by the transcriptional upregulation of *ppara* itself and several downstream target genes such as *pltp* and *cpt1*. Overall, PPARα did not seem to have any influence on the immune response against *G. muris*, since PPARα KO animals expressed *il-17a* and could clear the infection similar to WT controls. In conclusion, this study shows for the first time the importance of IL-17 production in the clearance of a *G. muris* infection together with an early induction of PPARα. The effect of the latter, however, is still unclear.

Adding up the 280 million human *Giardia duodenalis* infections a year to the high prevalences found in production animals and companion animals (1), it is clear that this protozoan is one of the most commonly found intestinal parasites in vertebrate hosts worldwide. *Giardia* has a simple direct life cycle that starts with the oral ingestion of infective cysts through contaminated food or water. Once it has passed through the stomach, excystation takes place with the release of flagellated trophozoites that rapidly colonize the mucosa of the small intestine without invading it. After the appropriate host signals, such as bile salts and a higher pH, trophozoites will encyst and thus form the infective cyst stage that is secreted with the feces (2).

The clinical manifestation of a *G. duodenalis* infection ranges from an asymptomatic carrier state to gastrointestinal complaints, such as diarrhea, weakness, weight loss, abdominal pain, and possibly nausea, vomiting, flatulence, and fever. Although in many cases the infection is acute and self-limiting, a significant proportion of humans will develop a chronic infection with intermittent diarrhea and cyst excretions lasting for several weeks or even months (3, 4). Finding the answer as to why exactly some infections remain chronic is hindered by our limited knowledge on the *in vivo* immune response in natural hosts. Recently, our group investigated the intestinal host response of calves infected with the ruminant-specific *G. duodenalis* assemblage E, which is characterized by the chronic nature of the infection (5). Using a bovine high-density microarray to analyze global gene transcription combined with histological work, the acute phase of the infection in cattle was marked by a lack of inflammation and immune cell infiltration. An upregulation of nuclear peroxisome proliferator-activated receptor alpha (PPARα) and gamma (PPARγ) gene expression was observed, which considering the anti-inflammatory potential of these receptors after activation (6), could possibly explain the chronicity of a *Giardia* infection in cattle. How exactly these receptors are activated following a *Giardia* infection is still unclear. Interestingly, after being incubated with *G. duodenalis* for 18 h, human intestinal Caco-2 cells showed an upregulation of PPARγ, suggesting that the same mechanism might also be active in humans (7).

On the basis of these results, we continued to gather insights by using a murine giardiasis model where mice are infected with their natural parasite, *Giardia muris*. The life cycle and infection process of this parasite are basically identical to those of *G. duodenalis*, with the only difference being that most mouse strains are able to clear a *G. muris* infection after 3 to 6 weeks of contact with the parasite (8). Earlier work already indicated the importance of CD4+ T cells (9, 10), B cells (11, 12), and IgG and IgA antibody production (13, 14) in the development of immunity. Work done

on the mucosal inflammatory response in *G. muris*-infected mice also suggested mast cells, mucous production, and gamma interferon (IFN-γ) as possible elements in the host response (15). However, further information regarding the type of immune response (Th1-Th2-Th17), regulatory pathways, and effector mechanisms involved, and finally, the dynamics of the whole immune development process is still missing. Therefore, the aim of the current study was to analyze cytokine transcription patterns and histological changes in the intestinal tissue at different time points during a *G. muris* infection in C57BL/6 mice, a strain that has the ability to control a *G. muris* infection. In addition, in order to further compare the responses in mice and cattle, we also investigated the potential activation of PPARs in the intestines of infected mice.

MATERIALS AND METHODS

Ethical statement. All animal experiments were conducted in accordance with the European Union (E.U.) Animal Welfare Directives and International Cooperation on Harmonization of Technical Requirements for Registration of Veterinary Medicinal Products (VICH) Guidelines for Good Clinical Practice, and ethical approval to conduct the studies was obtained from the Ethical Committee of the Faculty of Veterinary Medicine, Ghent University (ethical committee approval numbers EC 2012/027, EC 2013/49, EC 2012/176 and EC 2013/50) who have also approved the study.

Mouse studies. In each trial or experiment, mice were infected orally with 10^3 *G. muris* suspended in 0.2 ml phosphate-buffered saline (PBS). *Giardia muris* cysts were obtained from M. Belosevic, University of Alberta, Edmonton, Canada. All mice used in the trials were bred under similar conditions.

A total of 4 trials were executed (Table 1). Infection trial 1 consisted of infected female C57BL/6 mice (Harlan Laboratories) and the appropriate negative controls (five mice per group for all groups). All animals were 6 weeks old at the time of infection. In this trial, cyst counts were performed daily, and intestinal samples were taken from the infected animals at weeks 1, 2, and 3 postinfection (p.i.) (*n* = 5 at each time point).

Infection trial 2 used infected female C57BL/6 mice. Starting day 1 p.i., 5 animals were necropsied daily until day 7 for intestinal samples. Every day, 2 negative controls were necropsied and pooled as one group at the end of the trial.

For infection trial 3, female interleukin 17 (IL-17) receptor A (IL-17RA) knockout (KO) (16) mice were used. These mouse lines have been crossed back into a C57BL/6J background for over five generations. These animals (*n* = 5) were infected for 3 weeks where cyst counts were counted daily and compared to the appropriate C57BL/6 wild-type (WT) controls (*n* = 5).

The final infection trial (infection trial 4) compared the course of infection in female PPARα KO mice (17) (of a 10 generations backcrossed C57BL/6N genetic background) to 5 C57BL/6 WT controls during 3 weeks of infection. To achieve this, 5 KO animals and 5 WT mice were infected with *G. muris* cysts after which cyst counts were performed daily for each animal.

Cyst counts. To monitor the course of a *G. muris* infection in all trials, cyst excretion in feces was measured as described previously by Roberts-Thomson and Mitchell (8). In summary, feces were collected from each mouse individually over a 2-h period and weighed. Next, the stool was homogenized with PBS and centrifuged at low speed over a 1 M sucrose gradient. The cysts in the top layer were further washed, resuspended in 1 ml of PBS, and counted by using a hemacytometer. Cyst excretion was then expressed as the number of cysts per gram of feces. In the PPARA KO trial, statistical analysis was done using GraphPad Prism software. All cyst counts from one animal were considered repeated measures, and a two-way repeated-measures analysis of variance (ANOVA) with Bonferroni

TABLE 1 Summary of mouse trials[a]

Trial	Objective	Strain	Trial duration (wk)	No. of animals	Time point of sampling p.i.[b]	Data analyzed[c]
1	Intestinal immune response	C57BL/6	3	15 infected mice and 5 negative controls	Wk 1, 2, and 3	Cyst excretion and intestinal cytokine levels
2	Early intestinal immune response	C57BL/6	1	35 infected mice and 14 negative controls	Daily, starting day 1 p.i. until day 7 p.i.	Intestinal cytokine levels
3	Effect of IL17A on the intestinal immune response	C57BL/6 IL17RA-KO	3	5 infected IL17RA KO mice and 5 infected controls	NA	Cyst excretion
4	Effect of PPARα deletion on the intestinal immune response	C57BL/6 PPARα KO	3	5 infected PPARα KO mice and 5 infected controls	NA	Cyst excretion

[a] All trials or experiments were done with 6-week-old female mice.
[b] Samples were taken from the small intestine for subsequent qRT-PCR analysis of the main cytokines. NA, not available.
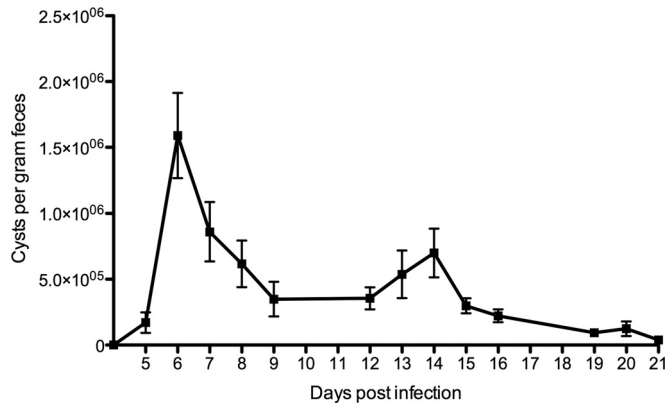[c] Cyst counts of feces were performed daily for each animal.

FIG 1 Cyst excretion pattern in C57BL/6 mice. Cysts excreted were counted daily using a sucrose density technique. Each point on the graph represents the mean cyst output per gram of feces for five animals ± standard error (error bar).
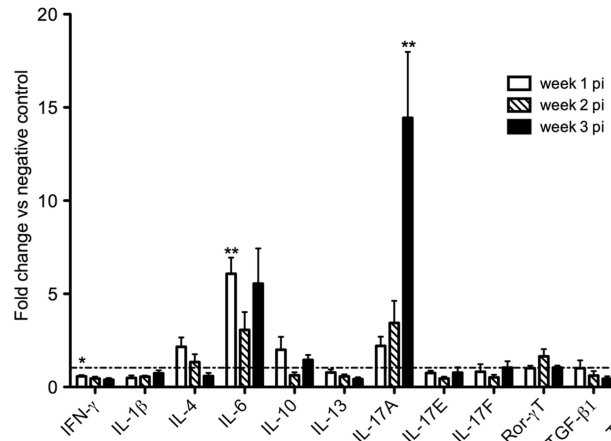

FIG 2 Cytokine transcription profile in the small intestines of *G. muris*-infected C57BL/6 mice. Transcription levels of the main cytokines were analyzed using quantitative PCR. Mean fold changes in infected mice (n = 5) compared to uninfected controls (dashed line) are presented, and standard errors of the means (SEM) are shown as error bars. Values that are significantly different are indicated by asterisks as follows: ∗∗, $P < 0.01$; ∗, $P < 0.05$.

posttest was used to calculate differences at every time point between the groups.

Tissue sample collection. At necropsy, 1-cm-long fragments of the small intestine were taken from each animal starting 4 cm from the gastroduodenal junction. To allow RNA extraction, the intestinal tissue was snap-frozen in liquid nitrogen and stored at −80°C.

RNA isolation and qRT-PCR. Total RNA was isolated by adding TRIzol (Invitrogen) to the snap-frozen tissue samples followed by an RNA purification with the RNeasy minikit (Qiagen). Any contaminating genomic DNA was removed with the help of the RNase-free DNase set (Qiagen) for on-column DNase digestion. An Experion automated electrophoresis system (Bio-Rad) was used to verify the quality of the isolated RNA, while total RNA concentrations were determined using a NanoDrop ND-1000 spectrophotometer (NanoDrop Technologies). To obtain the cDNA samples needed for quantitative real-time PCR (qRT-PCR), the iScript cDNA synthesis kit was used following the manufacturer's instructions.

All qRT-PCR analyses were carried out using the SYBR green master mix (Applied Biosystems), with 2 μl of single-stranded cDNA (10 ng of the input total RNA equivalent) and 500 nM amplification primer in a reaction mixture volume of 20 μl. The primer sets for amplification of the different genes were designed using Primer3 software (http://bioinfo.ut.ee/primer3-0.4.0/primer3/) and are listed in Table S1 in the supplemental material.

All qRT-PCR analyses were run on a StepOnePlus real-time PCR system (Applied Biosciences) with the following amplification cycles: 95°C for 20 s; 35 cycles, with 1 cycle consisting of 5 s at 95°C and 30 s at 60°C (the optimal annealing temperature for all the genes examined). Reaction efficiencies were measured based on a standard dilution curve obtained by serial dilutions of pooled cDNA material from all the samples. In every assay, a nontemplate control was added, and cDNA samples were analyzed in duplicate. At the end of the reactions, melting curve analyses were performed to ensure the specificity of the primers. The ΔC_T method was applied to transform the obtained threshold cycle (C_T) values in relative quantities. With this method, the following formula was used: $Q = E^{\text{min } Ct - \text{sample } Ct}$ where Q represents sample quantity relative to the sample with highest transcription, E represents amplification efficiency, min Ct is equal to the lowest C_T value, and sample Ct is the C_T value of the sample with the highest transcription level. The quantities obtained were then normalized against internal control genes, referred to as housekeeping genes (HKGs). Out of a panel of 6 candidate genes (beta actin [*ACTB*], hypoxanthine phosphoribosyltransferase 1 [*HPRT1*], ribosomal protein P0 [*RPLP0*], succinate dehydrogenase flavoprotein subunit A [*SDHA*], TATA box binding protein [TBP]-associated factor [*TAF2*], and ubiqui-

tin-conjugating enzyme E2D2 [*UBE2D2*]) (18), the most stable HKGs were selected based on the gene stability measure M calculated by the GeNorm software (geNorm3.5) (19). The eventual gene expression normalization factor for each animal sample was calculated based on the geometric mean of the two selected HKGs. This resulted in the use of HPRT1 and TBP as HKGs during the different trials. Gene expression was evaluated based on fold differences in gene transcription levels compared to the levels in negative-control animals. This was done by calculating the ratios of individual relative quantities on the geometric means of relative values of the control samples.

Statistical analysis was carried out using GraphPad Prism software. A one-way ANOVA followed by a Dunn's multiple-comparison test was used to determine differences between the infected group and the control group. A P value of ≤0.05 was considered significant.

Histology. To determine the presence of trophozoites in the small intestine, the tissue samples were stained with hematoxylin and eosin (H&E).

RESULTS

Analysis of the intestinal immune response in infected mice reveals IL-17A upregulation. In the first experiment, we analyzed the intestinal immune response in orally *G. muris*-infected C57BL/6 mice. The daily fecal cyst excretion of the individual animals (Fig. 1) revealed an infection pattern similar to those previously described in the literature (20), with a peak number of cysts around day 6 postinfection. Afterwards, cyst shedding rapidly declined until only low numbers could be found by week 3 p.i.

Next, we compared the gene transcription of a panel of cytokines in infected animals to noninfected controls. A qRT-PCR analysis revealed a transcriptional upregulation of *Il-17a* (Fig. 2), starting week 1 p.i. but most striking and statistically significant at week 3. Except for *Il6* at week 1 p.i., no other cytokine showed a significantly upregulated gene expression in infected animals compared to negative controls. A significant downregulated transcription could be seen for *ifng* at week 3 p.i. in infected animals compared to controls. In addition, downregulation could be seen for *tnfa* mRNA at week 1 p.i.

It is noted in the literature that the production of IL-17 in mice usually occurs in the presence of IL-6 and transforming growth
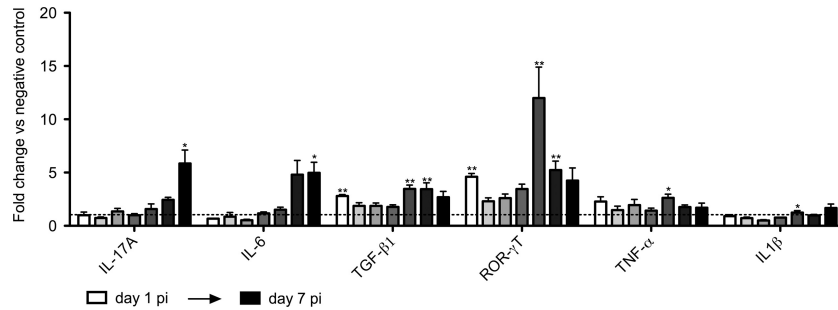
FIG 3 Transcription profile of cytokines in the small intestines of *G. muris*-infected C57BL/6 mice during the first days postinfection. The transcription profile of cytokines was analyzed starting day 1 p.i. up to day 7 p.i. Mean fold changes in infected mice ($n = 5$) compared to uninfected controls are presented, and SEM are shown as error bars. Values that are significantly different are indicated by asterisks as follows: ∗∗, $P < 0.01$; ∗, $P < 0.05$.

factor β (TGF-β). However, these cytokines were not found to be significantly upregulated at week 1, 2, or 3 p.i., with the exception of *Il-6* at week 1. We hypothesized that these cytokines upstream of IL-17 may appear earlier on in the infection. We decided to investigate this more closely and to set up a new infection trial in which the intestinal response was analyzed daily starting day 1 p.i. As a result, *Il-6* and *Tgfb1* were both found to be significantly upregulated preceding or coinciding with the *Il-17a* upregulation that started at day 6 p.i. (Fig. 3). In line with its regulatory role, the transcription factor *Rorc* showed higher transcription in the infected animals than in the controls at the earlier time points.

IL-17 is required for clearance of *G. muris*. Production of IL-17A in the intestine has been described before as critical in host defense against a number of infections such as extracellular bacteria (reviewed in reference 21). To demonstrate whether the transcriptional upregulation of IL-17A is important in the immunity against *G. muris*, a new infection experiment was set up in mice deficient for IL-17 receptor A (IL-17RA) (22). After infection of the IL-17RA KO animals and C57BL/6 wild-type controls, cumulative cyst counts were significantly higher in the KO animals than in the controls (Fig. 4A). This effect persisted throughout the whole 3-week duration of the study, after which WT animals were largely able to clear their infections, while high numbers of cysts persisted in KO animals. In addition, to determine the influence of IL-17A production on the trophozoites of *G. muris* present in the gut lumen, samples were taken from the small intestines of all animals at day 21 p.i. for further histological examination. Hematoxylin-and-eosin staining (Fig. 4B and C) revealed that in all WT animals, only a few trophozoites could be found after thorough microscopic examination of the whole slide, while a thick layer of trophozoites was still visible in the lumen of all the IL-17RA KO mice, indicating that the observed cyst counts are a result of the high number of trophozoites remaining in the gut lumen under circumstances where IL-17A is unable to execute its function.

As a first step toward unraveling the effector mechanisms downstream of IL-17A, qRT-PCRs were performed to examine the transcription of six antimicrobial peptides and proteins: β-defensins DEFB2 and DEFB3, Reg3γ, calprotectins S100A8 and S100A9, and cathelicidin. Upregulated transcription, although not significant, could be seen for both calprotectins S100A8 and S100A9 at week 1 p.i. (Fig. 5). From the remaining genes analyzed, cathelicidin was not differently expressed compared to control animals and for the β-defensins and Reg3γ, no transcripts could be amplified or detected in any of the samples.

Peroxisome proliferator-activated receptor alpha (PPARα) gene transcription is upregulated early on in infection. Our previous work identified upregulated PPARA and PPARG transcription as a possible reason for the chronicity of a *G. duodenalis* infection in cattle, keeping in mind the anti-inflammatory properties that are often attributed to these receptors (23). This prompted the question whether these receptors also show a higher gene expression in *G. muris*-infected mice. A qRT-PCR analysis was used to check the transcription profile of both *Pparg* (gamma) and *Ppara* (Fig. 6). No upregulation could be seen whatsoever for
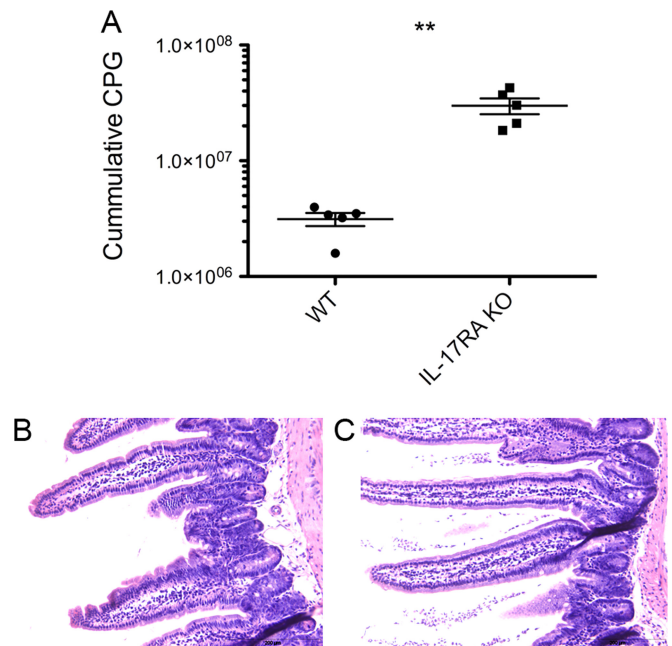

FIG 4 Cyst secretion and presence of trophozoites in *G. muris*-infected IL17RA KO animals and wild-type controls. To analyze the effect of the observed *il17a* upregulation, an infection trial was set up comparing IL17RA KO animals to infected wild-type controls. (A) Mean cumulative cyst output per gram of feces (CPG) for five animals. Each symbol represents the value for an individual mouse. The means ± standard errors for the animals in the two groups are indicated by the horizontal black line and error bars, respectively. The values for WT and IL17RA KO mice were significantly different ($P < 0.01$) as indicated by the asterisks. (B and C) HE staining illustrate the lack of trophozoites in the intestinal lumen of wild-type controls at week 3 p.i. (B), while high numbers of trophozoites were still visible in the intestinal lumen of the KO animals (C).
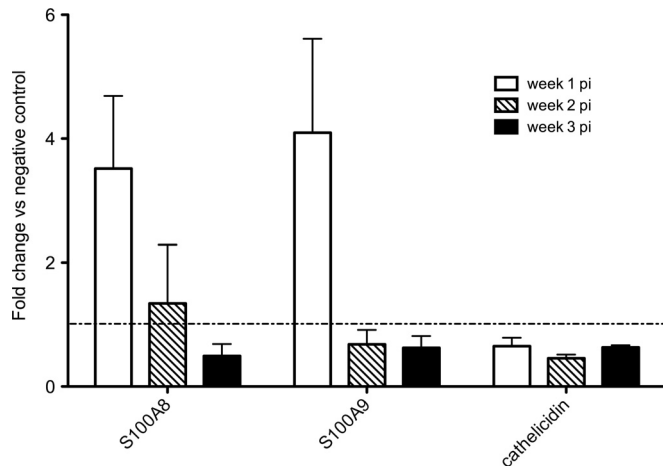
FIG 5 Transcription profile of antimicrobial proteins in the small intestines of *G. muris*-infected C57BL/6 mice. Transcription levels of antimicrobial proteins were analyzed using quantitative PCR. Mean fold changes in infected mice ($n = 5$) compared to uninfected controls are presented, and SEM are shown as error bars.

FIG 6 Transcription profile of peroxisome proliferator-activated receptors PPARα and PPARγ in small intestines of *G. muris*-infected C57BL/6 mice. Transcription levels of PPARγ and PPARα were analyzed using quantitative PCR. Mean fold changes in infected mice ($n = 5$) compared to uninfected controls are presented, and SEM are shown as error bars.

pparg. Concerning *Ppara*, C57BL/6 mice showed upregulation bordering the 2-fold threshold at week 1 p.i. and over 2-fold at weeks 2 and 3, although not statistically significant.

Additional qRT-PCR analyses of *Ppara* were done on the intestinal samples collected daily starting day 1 p.i. up until day 7 p.i. This indicated a transcriptional upregulation of *Ppara* from day 1 p.i. onwards in the infected animals compared to the negative controls (Fig. 7). To investigate whether the upregulation of *Ppara* expression also results in a functional PPARα activation, three genes (pyruvate dehydrogenase kinase, isozyme 4 [*Pdk4*]; carnitine palmitoyltransferase 1a [*Cpt1*]; and phospholipid transfer protein [*pltp*]) that are known downstream targets of PPARα (24) (typically measured in liver samples) were included in the qRT-PCR analysis. Again, upregulation was observed for two of the downstream target genes, with a significant upregulation of *pdk4* and *pltp* mRNA levels starting day 1 p.i., suggesting that the observed *Ppara* upregulation could indeed be linked to a functional PPARα activation.

PPARα does not influence immune development against *G. muris*. To further unravel the influence of PPARα on *G. muris* infection, we compared the time course of infection between WT and PPARα KO C57BL/6 mice by counting the cysts excreted by mice in both groups. To achieve this, cysts were counted daily starting day 5 p.i. up to week 3 p.i. Overall, no clear difference could be seen in the amount and duration of cyst excretion apart from day 5 p.i., when cyst excretion in the KO animals was higher than what was seen in the control mice (Fig. 8A) and the opposite effect on days 7 and 8 p.i., although the difference was statistically significant only for day 8. To investigate whether cyst excretion occurred earlier than day 5 p.i. in the PPARα KO mice, a second experiment was performed in which cyst excretion was measured daily starting from day 1 p.i. until day 7 p.i. The results of this experiment are shown in Fig. 8B. As in the first experiment, cyst excretion was detectable from day 5 p.i. onwards in the PPARα KO mice, whereas cyst excretion in the WT animals started from day 6 p.i. onwards. On day 7, however, no more difference could be seen between the groups. Quantitative RT-PCR analyses in
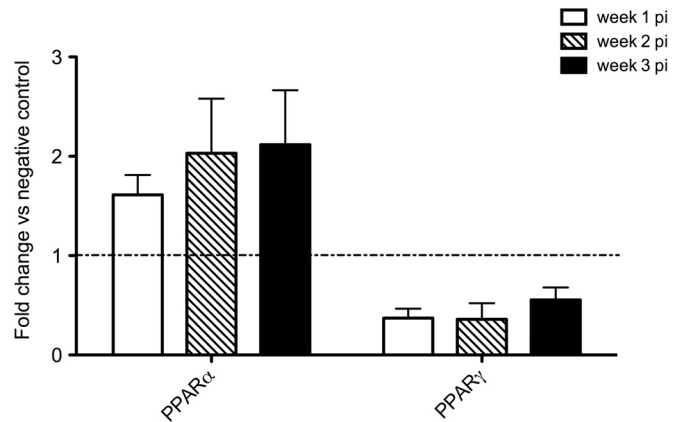
both the WT and KO mice revealed that after deletion of PPARα, *il17a* transcription was still significantly upregulated at weeks 1 and 3 p.i. in KO mice compared to uninfected negative controls. The WT animals that were included in this study again showed the upregulated expression of Il-17A that was observed in the earlier trials at both week 1 and statistically significant at week 3 p.i. with fold changes of 7 and 11, respectively, compared to WT negative controls (data not shown).

DISCUSSION

In this study, the general intestinal immune response in mice following a *G. muris* infection was investigated. The most prominent finding was the induction of IL-17A following infection, as measured by transcript levels by qRT-PCR. The highest transcriptional upregulation was repeatedly observed at week 3 postinfection. Although some variation was observed between the different experiments, the data indicated that IL-17A induction occurred from approximately 1 week p.i. onwards. In addition, when the functioning of this cytokine was impaired by deletion of IL-17RA, infected animals could no longer dispose of the parasite. In the absence of littermate IL-17RA$^{+/+}$ control mice, infection levels in the IL-17RA KO mice were compared to wild-type C57BL/6 mice. Although mice from different litters potentially have a different gut microbiome, it is unlikely that this is causing the lack of immune development in the IL-17RA KO mice. Analysis of cyst secretions in WT C57BL/6 mice from different origins and in BALB/c mice all showed a similar pattern, with the infection almost disappearing at 3 weeks p.i. (results not shown), which is totally different from the pattern observed in the IL-17RA KO mice.

To our knowledge, this is the first time that IL-17 production in the intestine is related to a protective immune response during a *G. muris* infection. Earlier work using the *G. muris* model did identify CD4$^+$ T cells as important elements in the clearance of the parasite, shown by the development of prolonged infections in nude mice (9) and mice depleted of T helper cells (10). Since these cells were not further characterized, the possibility remains that these were CD4$^+$ Th17 cells. Interestingly, when looking at *G. duodenalis*, an earlier study reported elevated production of IL-17
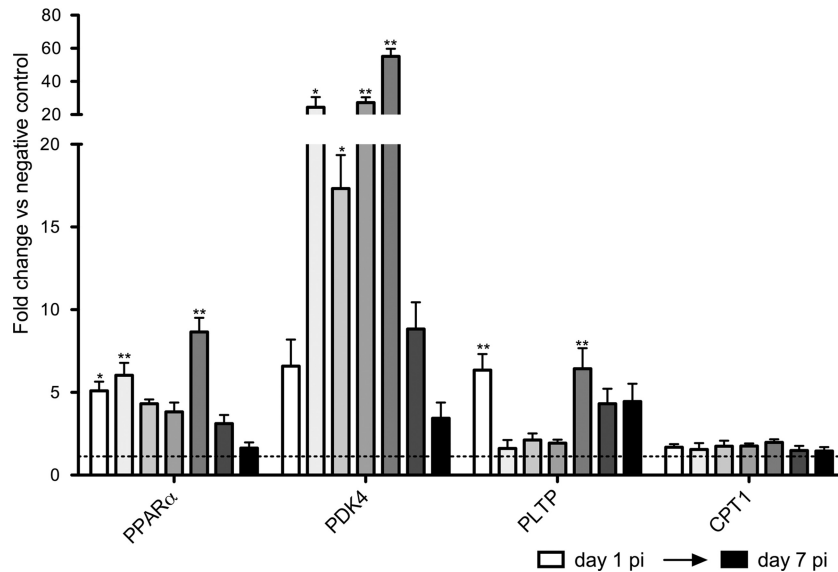
FIG 7 Transcription profile of PPARα and the main downstream target genes in the small intestines of *G. muris*-infected C57BL/6 mice during the first days postinfection. The transcription profile of PPARα and the main downstream target genes was analyzed starting day 1 p.i. up to day 7 p.i. Mean fold changes in infected mice ($n = 5$) compared to uninfected controls are presented, and SEM are shown as error bars. Values that are significantly different are indicated by asterisks as follows: ∗∗, $P < 0.01$; ∗, $P < 0.05$.
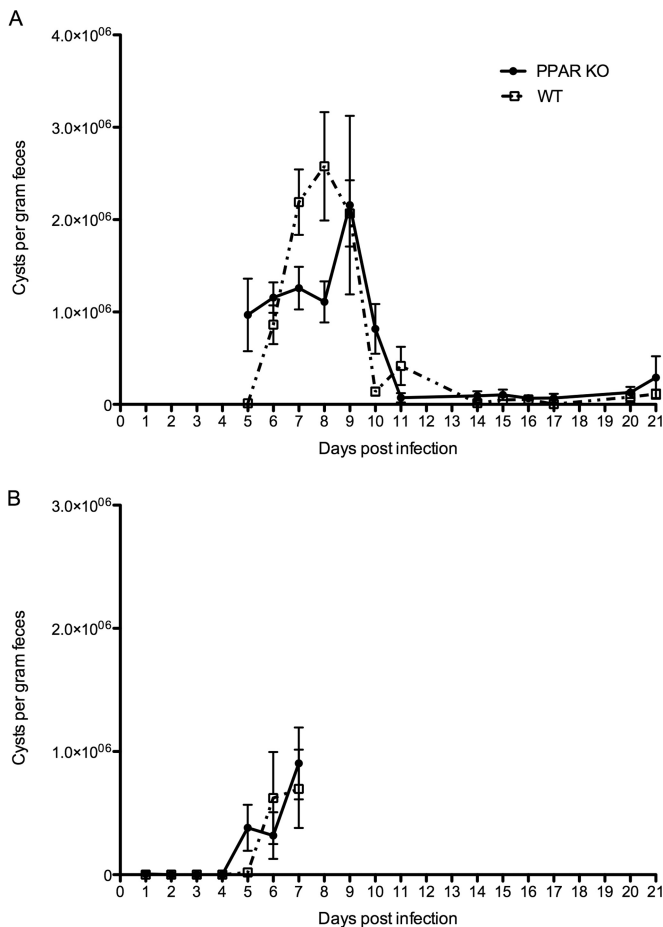

FIG 8 Comparison of infected PPARα KO mice and WT controls. (A) Cyst counts of the first trial where counting started at day 5 p.i.; (B) results of the second trial where counting was done daily starting day 1 p.i. until day 7 p.i. Each point on the graph represents the mean cyst output per gram of feces for 5 animals ± standard error.

in murine spleen and mesenteric lymph node cells in response to *G. duodenalis* extract (25), suggesting that an IL-17 response could be a typical anti-*Giardia* response in mice. In addition, cattle infected with *G. duodenalis* showed systemic IL-17 production after approximately 7 to 9 weeks of infection (26), at a time when protective immunity develops. Importantly, it should be noted that IL-17RA not only functions as a receptor for IL-17A but is also important for IL-17E and IL-17F signaling. The latter two cytokines, however, never showed upregulated transcription in infected mice compared to the controls.

Interleukin 17 is a cytokine that can be produced by cells that are part of both the innate and adaptive immune systems. In the mouse gut, high numbers of CD4^{+} Th17 cells are already present at steady state. Differentiation of the Th17 cells is directed by retinoic acid-related orphan receptor RORγT and driven by the cytokines IL-6 and TGF-β (27), all of which were found to have higher gene expression early on in the infection of C57BL/6 mice. In addition, work done by Bienz et al. (28) and Zhou et al. (29) has revealed that IL-6 plays an important role in controlling acute *G. duodenalis* infections in mice. However, conventional Th17 cells are not the only cells in the intestine capable of IL-17A production. In the gut, RORγT[+] γδ T cells are an innate source of IL-17 and can be directly activated by Toll-like receptors (TLRs) (27). Other possible RORγT^{+} sources of IL-17 include CD8^{+} αβ T cells, invariant natural killer cells, lymphoid tissue inducer (LTi), and LTi-like cells. Finally, mast cells, macrophages, and paneth cells can also be cellular sources of IL-17A (reviewed in reference 30). Since immunohistological staining for IL-17A performed on the intestinal tissue samples in this study was not successful, further research is needed to identify the cellular source of IL-17A following *G. muris* infections, for example by infecting RORγT-green fluorescent protein (GFP)-expressing mice with *G. muris* and subsequently identifying the cellular source by flow cytometry.

The role of IL-17 in the intestine has been described as dual, as

it can work in both a protective and pathological manner. The way it serves as an effector cytokine during the clearance of a *G. muris* infection still needs to be examined further. A possible explanation is the stimulation of mucin and defensin production by IL-17 (31, 32), both of which were earlier described as candidate defense mechanisms during *G. duodenalis* infection (reviewed in reference 33). In our study, however, no significant changes could be observed in the levels of expression of six antimicrobial peptides and proteins that are under the control of IL-17A (i.e., β-defensins, Reg3γ, cathelicidin, and calprotectin), suggesting that other factors are likely in play.

The levels of expression of PPARα and PPARγ in infected mice were also measured in this study, based on earlier work in calves. As mentioned before, the PPARs can exert a suppressive effect on the immune response. We previously hypothesized that this effect might cause a chronic infection in calves infected with *G. duodenalis*, since a lack of immune response was seen together with an upregulated gene expression of PPARα and PPARγ in these animals. The qRT-PCR analysis showed that PPARα mRNA, but not PPARγ mRNA, was indeed upregulated in infected mice as soon as day 1 p.i. The exact mechanism by which PPARα is induced and activated during an infection is still unclear, since a variety of ligands produced by the host or the parasite could be responsible (discussed in reference 5).

The outcome of the PPARα KO experiment indicated that PPARα did not exert any influence on the duration of an infection, since the KO animals were able to clear the infection after approximately 3 weeks, similar to the WT mice. Furthermore, cyst secretion during this 3-week period was not majorly affected by the absence of PPARα, although higher cyst excretion was repeatedly observed on day 5 p.i. in the KO animals compared to WT mice. How PPARα might influence cyst production early in the infection is still unclear, but it is possible that the levels of cholesterol, bile acids, and bile salts in the intestinal lumen have a role in this. All these factors have shown to influence *Giardia* encystation (34) and can be under the control of PPARα (35).

Whether PPARα activation has any influence on the kinetics of the IL-17A response early in infection is still unclear, but it is interesting to note that the IL-17A production starts only when the PPARα activation is largely over. However, the deletion of PPARα does not seem to have a great effect on IL-17A expression, considering that *il17a* still showed upregulated expression in PPARα KO animals. Further research is needed to unravel the potential regulatory role of PPARα in the IL-17 response.

In contrast to PPARα, the suppressive effect of PPARγ on Th17 responses has already been reported in several studies (36–38). Furthermore, earlier work in *G. duodenalis*-infected cattle revealed upregulation of PPARγ together with significant downregulation of IL-17A. Since no upregulated PPARγ expression was observed in *G. muris*-infected mice, it would be interesting to adopt a reverse strategy by inducing and activating PPARγ in mice and subsequently monitor possible effects on *G. muris* and immune development. Unfortunately, initial experiments with agonists failed to upregulate *pparg* transcription in the intestines of mice (results not shown).

In summary, this study revealed an early induction of PPARα followed by a protective IL-17A response in the intestines of *G. muris*-infected mice. Further research is now needed to further elucidate the cells and mechanisms involved in the induction and regulatory functions of both PPARα and IL-17A.

REFERENCES

1. **Geurden T, Vercruysse J, Claerebout E.** 2010. Is Giardia a significant pathogen in production animals? Exp. Parasitol. **124:**98–106. http://dx.doi.org/10.1016/j.exppara.2009.03.001.
2. **Farthing MJ.** 1996. Giardiasis. Gastroenterol. Clin. North Am. **25:**493–515. http://dx.doi.org/10.1016/S0889-8553(05)70260-0.
3. **Rendtorff RC.** 1954. The experimental transmission of human intestinal protozoan parasites. II. Giardia lamblia cysts given in capsules. Am. J. Hyg. **59:**209–220.
4. **Robertson LJ, Hanevik K, Escobedo AA, Morch K, Langeland N.** 2010. Giardiasis–why do the symptoms sometimes never stop? Trends Parasitol. **26:**75–82. http://dx.doi.org/10.1016/j.pt.2009.11.010.
5. **Dreesen L, Rinaldi M, Chiers K, Li R, Geurden T, Van den Broeck W, Goddeeris B, Vercruysse J, Claerebout E, Geldhof P.** 2012. Microarray analysis of the intestinal host response in Giardia duodenalis assemblage E infected calves. PLoS One **7:**e40985. http://dx.doi.org/10.1371/journal.pone.0040985.
6. **Daynes RA, Jones DC.** 2002. Emerging roles of PPARs in inflammation and immunity. Nat. Rev. Immunol. **2:**748–759. http://dx.doi.org/10.1038/nri912.
7. **Roxstrom-Lindquist K, Ringqvist E, Palm D, Svard S.** 2005. Giardia lamblia-induced changes in gene expression in differentiated Caco-2 human intestinal epithelial cells. Infect. Immun. **73:**8204–8208. http://dx.doi.org/10.1128/IAI.73.12.8204-8208.2005.
8. **Roberts-Thomson IC, Mitchell GF.** 1978. Giardiasis in mice. I. Prolonged infections in certain mouse strains and hypothymic (nude) mice. Gastroenterology **75:**42–46.
9. **Stevens DP, Frank DM, Mahmoud AA.** 1978. Thymus dependency of host resistance to Giardia muris infection: studies in nude mice. J. Immunol. **120:**680–682.
10. **Heyworth MF, Carlson JR, Ermak TH.** 1987. Clearance of Giardia muris infection requires helper/inducer T lymphocytes. J. Exp. Med. **165:**1743–1748. http://dx.doi.org/10.1084/jem.165.6.1743.
11. **Snider DP, Skea D, Underdown BJ.** 1988. Chronic giardiasis in B-cell-deficient mice expressing the xid gene. Infect. Immun. **56:**2838–2842.
12. **Skea DL, Underdown BJ.** 1991. Acquired resistance to Giardia muris in X-linked immunodeficient mice. Infect. Immun. **59:**1733–1738.
13. **Heyworth MF.** 1986. Antibody response to Giardia muris trophozoites in mouse intestine. Infect. Immun. **52:**568–571.
14. **Daniels CW, Belosevic M.** 1994. Serum antibody responses by male and female C57Bl/6 mice infected with Giardia muris. Clin. Exp. Immunol. **97:**424–429.
15. **Venkatesan P, Finch RG, Wakelin D.** 1997. A comparison of mucosal inflammatory responses to Giardia muris in resistant B10 and susceptible BALB/c mice. Parasite Immunol. **19:**137–143. http://dx.doi.org/10.1046/j.1365-3024.1997.d01-189.x.
16. **Flierl MA, Rittirsch D, Gao H, Hoesel LM, Nadeau BA, Day DE, Zetoune FS, Sarma JV, Huber-Lang MS, Ferrara JL, Ward PA.** 2008. Adverse functions of IL-17A in experimental sepsis. FASEB J. **22:**2198–2205. http://dx.doi.org/10.1096/fj.07-105221.
17. **Lee SS, Pineau T, Drago J, Lee EJ, Owens JW, Kroetz DL, Fernandez-Salguero PM, Westphal H, Gonzalez FJ.** 1995. Targeted disruption of the alpha isoform of the peroxisome proliferator-activated receptor gene in mice results in abolishment of the pleiotropic effects of peroxisome proliferators. Mol. Cell. Biol. **15:**3012–3022.
18. **Wang F, Wang J, Liu D, Su Y.** 2010. Normalizing genes for real-time polymerase chain reaction in epithelial and nonepithelial cells of mouse small intestine. Anal. Biochem. **399:**211–217. http://dx.doi.org/10.1016/j.ab.2009.12.029.
19. **Andersen CL, Jensen JL, Orntoft TF.** 2004. Normalization of real-time quantitative reverse transcription-PCR data: a model-based variance estimation approach to identify genes suited for normalization, applied to bladder and colon cancer data sets. Cancer Res. **64:**5245–5250. http://dx.doi.org/10.1158/0008-5472.CAN-04-0496.
20. **Belosevic M, Faubert GM, Skamene E, MacLean JD.** 1984. Susceptibility and resistance of inbred mice to Giardia muris. Infect. Immun. **44:**282–286.
21. **Korn T, Bettelli E, Oukka M, Kuchroo VK.** 2009. IL-17 and Th17 cells.

Annu. Rev. Immunol. **27**:485–517. http://dx.doi.org/10.1146/annurev
.immunol.021908.132710.

22. **Ye P, Rodriguez FH, Kanaly S, Stocking KL, Schurr J, Schwarzenberger
    P, Oliver P, Huang W, Zhang P, Zhang J, Shellito JE, Bagby GJ, Nelson
    S, Charrier K, Peschon JJ, Kolls JK.** 2001. Requirement of interleukin 17
    receptor signaling for lung CXC chemokine and granulocyte colony-
    stimulating factor expression, neutrophil recruitment, and host defense. J.
    Exp. Med. **194**:519–527. http://dx.doi.org/10.1084/jem.194.4.519.

23. **Delerive P, Fruchart JC, Staels B.** 2001. Peroxisome proliferator-
    activated receptors in inflammation control. J. Endocrinol. **169**:453–459.
    http://dx.doi.org/10.1677/joe.0.1690453.

24. **Lefebvre P, Chinetti G, Fruchart JC, Staels B.** 2006. Sorting out the roles
    of PPAR alpha in energy metabolism and vascular homeostasis. J. Clin.
    Invest. **116**:571–580. http://dx.doi.org/10.1172/JCI27989.

25. **Solaymani-Mohammadi S, Singer SM.** 2011. Host immunity and patho-
    gen strain contribute to intestinal disaccharidase impairment following
    gut infection. J. Immunol. **187**:3769–3775. http://dx.doi.org/10.4049
    /jimmunol.1100606.

26. **Grit G, Van Coppernolle S, Devriendt B, Geurden T, Dreesen L, Hope
    J, Vercruysse J, Cox E, Geldhof P, Claerebout E.** 2014. Evaluation of
    cellular and humoral systemic immune response against Giardia duode-
    nalis infection in cattle. Vet. Parasitol. **202**:145–155. http://dx.doi.org/10
    .1016/j.vetpar.2014.03.012.

27. **Gibbons DL, Spencer J.** 2011. Mouse and human intestinal immunity:
    same ballpark, different players; different rules, same score. Mucosal Im-
    munol. **4**:148–157. http://dx.doi.org/10.1038/mi.2010.85.

28. **Bienz M, Dai WJ, Welle M, Gottstein B, Muller N.** 2003. Interleukin-
    6-deficient mice are highly susceptible to Giardia lamblia infection but
    exhibit normal intestinal immunoglobulin A responses against the para-
    site. Infect. Immun. **71**:1569–1573. http://dx.doi.org/10.1128/IAI.71.3
    .1569-1573.2003.

29. **Zhou P, Li E, Zhu N, Robertson J, Nash T, Singer SM.** 2003. Role of
    interleukin-6 in the control of acute and chronic Giardia lamblia infec-
    tions in mice. Infect. Immun. **71**:1566–1568. http://dx.doi.org/10.1128
    /IAI.71.3.1566-1568.2003.

30. **Morrison PJ, Ballantyne SJ, Kullberg MC.** 2011. Interleukin-23 and T
    helper 17-type responses in intestinal inflammation: from cytokines to
    T-cell plasticity. Immunology **133**:397–408. http://dx.doi.org/10.1111/j
    .1365-2567.2011.03454.x.

31. **Ishigame H, Kakuta S, Nagai T, Kadoki M, Nambu A, Komiyama Y,
    Fujikado N, Tanahashi Y, Akitsu A, Kotaki H, Sudo K, Nakae S,
    Sasakawa C, Iwakura Y.** 2009. Differential roles of interleukin-17A and
    -17F in host defense against mucoepithelial bacterial infection and allergic
    responses. Immunity **30**:108–119. http://dx.doi.org/10.1016/j.immuni
    .2008.11.009.

32. **Chen Y, Thai P, Zhao YH, Ho YS, DeSouza MM, Wu R.** 2003. Stimu-
    lation of airway mucin gene expression by interleukin (IL)-17 through
    IL-6 paracrine/autocrine loop. J. Biol. Chem. **278**:17036–17043. http://dx
    .doi.org/10.1074/jbc.M210429200.

33. **Muller N, von Allmen N.** 2005. Recent insights into the mucosal reac-
    tions associated with Giardia lamblia infections. Int. J. Parasitol. **35**:1339–
    1347. http://dx.doi.org/10.1016/j.ijpara.2005.07.008.

34. **Adam RD.** 2001. Biology of Giardia lamblia. Clin. Microbiol. Rev. **14**:
    447–475. http://dx.doi.org/10.1128/CMR.14.3.447-475.2001.

35. **Post SM, Duez H, Gervois PP, Staels B, Kuipers F, Princen HM.** 2001.
    Fibrates suppress bile acid synthesis via peroxisome proliferator-activated
    receptor-alpha-mediated downregulation of cholesterol 7alpha-
    hydroxylase and sterol 27-hydroxylase expression. Arterioscler. Thromb.
    Vasc. Biol. **21**:1840–1845. http://dx.doi.org/10.1161/hq1101.098228.

36. **Viladomiu M, Hontecillas R, Pedragosa M, Carbo A, Hoops S, Micha-
    lak P, Michalak K, Guerrant RL, Roche JK, Warren CA, Bassaganya-
    Riera J.** 2012. Modeling the role of peroxisome proliferator-activated
    receptor gamma and microRNA-146 in mucosal immune responses to
    Clostridium difficile. PLoS One **7**:e47525. http://dx.doi.org/10.1371
    /journal.pone.0047525.

37. **Klotz L, Burgdorf S, Dani I, Saijo K, Flossdorf J, Hucke S, Alferink J,
    Nowak N, Beyer M, Mayer G, Langhans B, Klockgether T, Waisman A,
    Eberl G, Schultze J, Famulok M, Kolanus W, Glass C, Kurts C, Knolle
    PA.** 2009. The nuclear receptor PPAR gamma selectively inhibits Th17
    differentiation in a T cell-intrinsic fashion and suppresses CNS autoim-
    munity. J. Exp. Med. **206**:2079–2089. http://dx.doi.org/10.1084/jem
    .20082771.

38. **Park SJ, Lee KS, Kim SR, Min KH, Choe YH, Moon H, Chae HJ, Yoo
    WH, Lee YC.** 2009. Peroxisome proliferator-activated receptor gamma
    agonist down-regulates IL-17 expression in a murine model of allergic
    airway inflammation. J. Immunol. **183**:3259–3267. http://dx.doi.org/10
    .4049/jimmunol.0900231.